Information-Energy Capacity Region for SLIPT Systems over Lognormal-Fading Channels

Kapila W. S. Palitharathna*, Nizar Khalfet*, Constantinos Psomas*, George K. Karagiannidis†‡, and Ioannis Krikidis*
*Department of Electrical and Computer Engineering, University of Cyprus, Nicosia, Cyprus
†Department of Electrical and Computer Engineering, Aristotle University of Thessaloniki, Thessaloniki, Greece
‡Artificial Intelligence & Cyber Systems Research Center, Lebanese American University (LAU), Lebanon
Email: {palitharathna.kapila, khalfet.nizar, psomas, krikidis}@ucy.ac.cy, geokarag@auth.gr

***Abstract*—In this paper, we study the fundamental limits of simultaneous lightwave information and power transfer (SLIPT) systems over channels with path loss and lognormal fading conditions. We consider a system with a single transmitter transferring information to a photodiode-based receiver as well as transferring energy to a photovoltaic cell receiver. In particular, we study the information-energy capacity region and the optimal input distribution under (a) peak-power and average-power constraints at the transmitter, and (b) the minimum harvest energy at the energy harvesting receiver. To this end, an expression for the transition probability distribution function of the lognormal channel is derived. By extending Smith's framework and using Hermite polynomial bases, we prove that the optimal input distribution is discrete with a finite number of mass points. Information-energy capacity region for SLIPT over lognormal channel conditions is illustrated and compared with the case of additive white Gaussian noise channel.**

***Index Terms*—Simultaneous lightwave information and power transfer, optimal input distribution, information-energy capacity region, lognormal channel.**

I. Introduction

Optical wireless communication (OWC) has been recognized as a promising technology to achieve high speed, low latency, and highly secure communication. Thanks to the use of the optical spectrum, OWC overcomes the current spectrum limitation of radio frequency (RF) technology, and hence is suitable for many applications in future wireless systems such as 6G networks. OWC has been categorized into many technologies depending on the application environment, such as free-space optical communication, visible light communication, light-fidelity, underwater optical wireless communication, and non-terrestrial satellite communication [1]. Light-emitting diodes (LEDs)/laser diodes (LD) are used as transmitters, while photodiodes (PD)/photovoltaic (PV) cells are used for receivers. Moreover, the existing lighting infrastructures can be easily adapted for simultaneous illumination, information transfer, and lightwave power transfer [1].

Recently, simultaneous lightwave information and power transfer (SLIPT) has emerged as a new communication paradigm that exploits optical signals for the dual purpose of information and energy transfer [2], [3]. Specifically, SLIPT is promising to charge batteries in energy-deprived devices/sensors efficiently, specifically in applications where other wireless charging methods are challenging, such as underwater, inter-satellite, vehicular, and indoor systems [3]. In the foundational analysis of SLIPT in [2], the maximization of energy transfer is considered while satisfying quality of service constraints. In [4], the minimum rate maximization and the transmit power minimization problems have been studied. Various SLIPT policies, receiver designs, and applications have been presented in [5]. The rate-power tradeoff in SLIPT has been studied in [6]. Moreover, SLIPT has been used in various use cases [7]–[9]. In [7], a beamforming design in a multi-cell setup has been investigated to maximize the data rate. In [8], resonant beams have been used to demonstrate highly efficient energy transfer. Finally, SLIPT has also been applied to underwater communication systems in [9].

It is well known that closed-form expressions for the exact capacity of OWC systems are unknown, and thus, several lower and upper bounds have been derived [10], [11]. Furthermore, the study of the information-energy capacity region of SLIPT has been limited, with a bound presented in [12]. Most of the aforementioned studies on SLIPT systems focus on simple additive white Gaussian noise (AWGN) channels with a static path loss, and therefore the impact of the channel fading on the optimal input distribution has not been investigated. However, SLIPT systems undergo fading effects and several fading models have been used in the literature, *i.e.*, lognormal, gamma-gamma, generalized gamma, and exponential gamma [13]. As a widely used fading model, the lognormal distributions have been used to model the fading in underwater weak turbulence conditions, over-the-air systems with fog/weak atmospheric turbulence conditions [13], [14]. Hence, it is crucial to study the exact information-energy capacity region and the optimal input distribution of SLIPT systems under lognormal fading conditions for future wireless system designs.

On the other hand, OWC transmitters are subjected to peak-power (PP) and average-power (AP) constraints. To avoid the non-linear distortions in the transmit signals, LED/LD needs to be operated in the linear operation range. This imposes a PP constraint on the transmit signal [10], [11]. Moreover, an AP constraint is required due to safety reasons (eye safety) and practical implementation limitations [11]. In SLIPT systems, the energy harvesting (EH) receiver is required to harvest a certain average harvest energy level in order to maintain the

This work has received funding from the European Research Council (ERC) under the European Union's Horizon 2020 research and innovation programme (Grant agreement No. 819819) and the European Union's Horizon Europe programme (ERC, WAVE, Grant agreement No. 101112697). Views and opinions expressed are however those of the author(s) only and do not necessarily reflect those of the European Union or the European Research Council Executive Agency. Neither the European Union nor the granting authority can be held responsible for them. This work was also supported by the Agence Universitaire de la Francophonie (AUF) under an Inter-university Scientific Cooperation project (PCSI).

2024 IEEE International Symposium on Information Theory (ISIT) | 979-8-3503-8284-6/24/$31.00 ©2024 IEEE | DOI: 10.1109/ISIT57864.2024.10619232

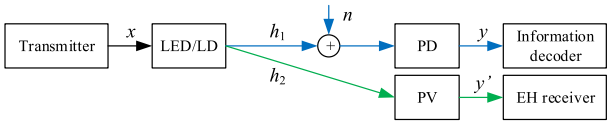

Fig. 1. A SLIPT system over a lognormal-fading channel with an LED/LD transmitter, a PD-based information decoder, and a PV cell EH receiver.

battery charging or to device operations, which impose an EH constraint [4]. Despite the use of the linear EH model in the literature [4], some papers focus on a nonlinear EH model [9], [12] that fit well with hardware requirements. To the best of the authors' knowledge, this is the first work that studies the information-energy capacity region and optimal input distribution of SLIPT systems with PP, AP, and EH constraints and nonlinear EH model over lognormal-fading channels from an information-theoretic standpoint.

This paper studies the information-energy capacity region for SLIPT systems over lognormal-fading channels. Specifically, a system that transmits data to an information receiver and lightwave power to an EH receiver using a single transmitter is considered. We consider a lognormal-fading channel with a path loss and consider PP, AP, and EH constraints. An expression for the transition probability distribution of the lognormal channel is derived. By using Smith's framework [15], a Hermite polynomial base, and the transition probability of the channel, we show that the optimal input distribution is discrete with a finite number of mass points. The information-energy capacity region of the considered system is illustrated and compared with the conventional AWGN channel.

II. System Model

We consider a SLIPT system over a lognormal channel, wherein the transmitter is comprised of a single, narrow-beam LED/LD. A PD receiver is used for information reception and a PV cell receiver is used for lightwave EH, as detailed in previous works [2], [3], [5]. The transmitter uses intensity modulation (IM), and hence, the instantaneous output optical power is proportional to the driving current signal. At the receiver, direct detection (DD) is used, and hence, a current is generated through the PD/PV cell that is proportional to the incident optical power. The generated current signals from the PD and the PV cell are separately sent for information decoding and EH. The harvested energy from the PV cell receiver can be used to charge a battery while the received signal from the PD is first sent through a trans-impedance amplifier to convert it to a voltage signal and then goes through the decoding stage [4]. A system diagram of this model is depicted in Fig. 1.

A. Channel Model

The channel gain from the LED/LD to the PD can be modeled using $h_1 = h_{1,l}h_T$, where $h_{1,l}$ is the path loss, and h_T is the lognormal distributed turbulence-induced fading. $h_{1,l}$ is deterministic and depends on the transmitter-receiver geometry. It can be expressed as [16]

$$h_{1,l} = \eta_t \eta_r e^{\frac{-c(\lambda)l}{\cos\theta_{PD}}} \frac{A_{PD}\cos\theta_{PD}}{2\pi l^2(1-\cos\theta_0)}, \quad (1)$$

where η_t and η_r are the optical efficiencies of the transmitter and receiver, respectively, $c(\lambda)$ is the extinction coefficient of the channel, λ is the optical wavelength, l is the perpendicular distance between the transmitter plane and the receiver plane, θ_0 is the transmitter beam divergence angle, θ_{PD} is the angle between the perpendicular axis to the receiver plane and the transmitter-PD trajectory, and A_{PD} is the PD aperture area.

The lognormal distribution is used to model the fading coefficient h_T in weak turbulence conditions in OWC, (*i.e.*, weak oceanic turbulence and weak atmospheric turbulence). Its probability density function (pdf) is given by [13], [17]

$$p_{h_T}(h_T) = \frac{1}{2h_T\sqrt{2\pi\sigma_{X_l}^2}} \exp\left(-\frac{(\ln h_T - 2\mu_{X_l})^2}{8\sigma_{X_l}^2}\right). \quad (2)$$

The fading coefficient in the above takes the form $h_T = e^{2X_l}$, where X_l is the fading log-amplitude, which is Gaussian distributed with mean μ_{X_l} and variance $\sigma_{X_l}^2$. Normalizing the fading coefficient to ensure that fading does not affect the average power leads to $\mu_{X_l} = -\sigma_{X_l}^2$. We assume that the channel gain between the LED/LD to the PV is static, and hence, it can be modeled as $h_2 = h_{2,l}$, where $h_{2,l}$ is the geometric path loss from the LED/PD transmitter to the PV cell receiver. It can be obtained by replacing A_{PD} and θ_{PV} in (1) with A_{PV} and θ_{PV}, respectively, where A_{PV} is the effective area of the PV cell and θ_{PV} is the angle between the perpendicular axis to the receiver plane and the transmitter-PV cell trajectory.

B. Information Transfer

We consider a memoryless discrete-time lognormal channel [18]. Let $x \in \mathbb{R}^+$ be the transmit signal. For a given $A > 0$, and $\varepsilon > 0$, its PP and AP constraints are $0 \le x \le A$, and $\mathbb{E}\{x\} \le \varepsilon$ [11]. The received electrical signal at the information receiver is expressed as

$$y = aR_P h_1 x + n, \quad (3)$$

where a is the electrical-to-optical conversion efficiency at the LED/LD, R_P is the responsivity of the PD, and n is the real AWGN with zero mean and variance σ_g^2, i.e., $n \sim \mathcal{N}(0, \sigma_g^2)$.

C. Power Transfer

To perform EH, the PV receiver generates a current from incident optical power and stores charges in a battery. The received current signal at the PV receiver is expressed as

$$y' = aR_E h_2 x, \quad (4)$$

where R_E is the responsivity of the PV cell. The effect of the noise can be neglected in PV cell receivers[1]. The harvested energy at the EH receiver for the time duration T is expressed as [2], [9]

$$E_H = f_E T I_s V_{oc}, \quad (5)$$

where f_E is the fill factor of the PV cell, I_s is the shunt current, and V_{oc} is the open circuit voltage. Within our

[1]In practical systems, the noise power at the PV receiver is negligible compared to the signal power [5].

mathematical framework, I_s is expressed as aR_Eh_2x, *i.e.*, the received current signal at the PV receiver, and V_{oc} is $v_t \ln\left(1+\frac{aR_Eh_2x}{I_0}\right)$, where v_t is the thermal voltage, and I_0 is the dark saturation current [2]. Combining these expressions and taking the expectation, the average harvest energy can be expressed as

$$\bar{E}_H = \mathbb{E}\left\{ f_E v_t T a R_E h_2 x \ln\left(1+\frac{aR_Eh_2x}{I_0}\right)\right\}. \quad (6)$$

To satisfy the EH requirement at the receiver, $\bar{E}_H$ needs to be greater than the given threshold value, E_{th}, *i.e.*, $E_{th} \leq \bar{E}_H$.

D. Problem Formulation

We form an optimization problem to maximize the mutual information between the channel input X and the channel output Y subject to PP and AP constraints at the transmitter, and a minimum harvested energy constraint at the EH receiver. The optimization problem is expressed as

$$\max_{F\in\mathcal{F}_A} \quad I(F) = \int_0^A \int_y p(y|x)\log_2\frac{p(y|x)}{p(y;F)}\mathrm{d}y\mathrm{d}F(x) \quad (7a)$$

$$\text{s.t.} \quad \mathbb{E}\{X\} \leq \varepsilon, \quad (7b)$$

$$\mathbb{E}\left\{bX\ln(1+cX)\right\} \geq E_{th}, \quad (7c)$$

where $b = f_E v_t T a R_E h_2$ and $c = aR_Eh_2/I_0$ are constants, $\mathcal{F}_A$ is the set of all input distributions that satisfy the PP constraint, i.e., $\mathcal{F}_A = \left\{F\in\mathcal{F}, \int_0^A \mathrm{d}F(x) = 1\right\}$, and $\mathcal{F}$ is the set of all possible input distributions. The mutual information between random variables X and Y of input and output, respectively, can be written as a function of the input distribution F,

$$I(F) \triangleq \int_0^A i(x;F)\mathrm{d}F(x), \quad (8)$$

where $i(x;F) = \int_y p(y|x)\log_2\frac{p(y|x)}{p(y;F)}\mathrm{d}y$ is the marginal information density. Denote by $g_j : F \to \mathbb{R}$ with $j\in\{1,2\}$ the following functions

$$g_1(F) \triangleq \int_0^A x\mathrm{d}F(x) - \varepsilon, \quad (9)$$

$$g_2(F) \triangleq E_{\text{th}} - \int_0^A bx\ln(1+cx)\mathrm{d}F(x), \quad (10)$$

and, let Ω be the set of all input distributions, such that

$$\Omega = \left\{F\in\mathcal{F}; \int_0^A dF(x) = 1; g_j(F)\leq 0; j\in\{1,2\}\right\}. \quad (11)$$

Hence, the optimization problem in (7) could be written in the compact form as $C = \sup_{F\in\Omega} I(F)$.

III. Optimal Input Distribution

We study the properties of the capacity-achieving distribution of the SLIPT system, the solution to the optimization problem in (7). To this end, the mathematical framework proposed in [15] is extended to the lognormal channel with a EH receiver. Firstly, Theorem 1 establishes the existence and the uniqueness of the optimal input distribution. Secondly, by using the Lagrangian Theorem, the dual equivalent problem is given by Corollary 1. Thirdly, we provide necessary and sufficient conditions for the optimal input distribution in Theorem 2 and extend to a more useful set in Corollary 2. Finally, we show that the capacity-achieving input distribution is discrete in Theorem 3.

Theorem 1. *The capacity C is achieved by a unique input distribution F^*, i.e.,*

$$C = \sup_{F\in\Omega} I(F) = I(F^*). \quad (12)$$

Proof. The proof follows a similar approach as in [18]. □

Corollary 1. *The strong duality holds for the optimization problem in* (12)*. i.e., there are constants, $\lambda_j \geq 0$, for $j\in\{1,2\}$ such that*

$$C = \sup_{F\in\Omega} I(F) - \sum_{j=1}^{2}\lambda_j g_j(F). \quad (13)$$

Proof. The proof follows a similar approach as in [18]. □

Theorem 2. *F^* is the capacity-achieving input distribution, if and only if, $\forall F\in\Omega$ there exist $\lambda_j > 0$, for $j\in\{1,2\}$ such that*

$$\int_0^A \left\{i(x;F^*) - \lambda_1 x + \lambda_2 bx\ln(1+cx)\right\}\mathrm{d}F(x) \leq C - \lambda_1\varepsilon + \lambda_2 E_{th}. \quad (14)$$

Proof. The proof follows a similar approach as in [19]. □

Corollary 2. *Let Supp(F^*) be the points of support of a distribution F^*. Then, F^* is the optimal input distribution, if there exist $\lambda_1 \geq 0$, and $\lambda_2 \geq 0$, such that*

$$\lambda_1(x-\varepsilon) - \lambda_2(bx\ln(1+cx) - E_{th}) + C - \int_y p(y|x)\log_2\frac{p(y|x)}{p(y;F^*)}\mathrm{d}y \geq 0, \quad (15)$$

for all x, with equality if $x\in$ Supp(F^*).

Proof. The proof follows a similar approach as in [19]. Due to the space limitations, we do not provide it here. □

In the following, we will show that the equality in Corollary 2 can not be satisfied in a set that has an accumulation point, hence the support of F^* must be discrete. The discretness property of the optimal input distribution is given by the following theorem,

Theorem 3. *The optimal input distribution that achieves the capacity in* (7) *is discrete with a finite number of mass points.*

Proof. The proof is presented in Appendix A. □

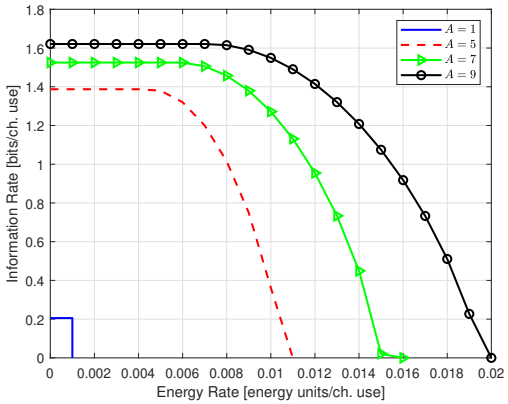

Fig. 2. Information-energy capacity region with different PP constraints; $P = 30$ dP

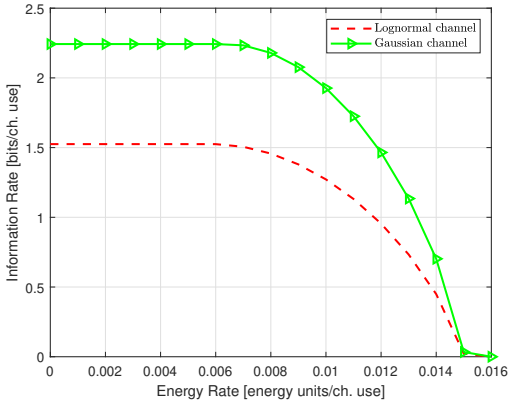

Fig. 3. Effect of the channel on the information-energy capacity region; $A = 7$, $P = 30$ dB.

IV. Numerical Results and Discussion

We characterized the optimal input distribution for a lognormal channel with AP, PP, and EH constraints. Now, we numerically evaluate the information-energy capacity region by using a numerical solver such as CVX [20]. Unless stated otherwise, the parameter values are set to, $a = 20$ W/A, $R_P = 0.5$ A/W, $R_E = 0.75$ A/W, $f_E = 0.5$, $T = 1$ s, $v_t = 25$ mV, $I_0 = 10^{-9}$ A, $\eta_t = \eta_r = 1$, $c(\lambda) = 0.03$ m^{-1}, $l = 10$ m, $\theta_0 = 10^\circ$, $\theta_{PD} = 0^\circ$, $\theta_{PV} = 5^\circ$, $A_{PD} = 0.001$ m^2, $A_{PV} = 0.01$ m^2, $E_{th} = 1$ mJ, $\sigma_g^2 = 10^{-12}$, and $\sigma_{X_t}^2 = 0.1$ [2], [4], [9].

Fig. 2 shows the information-energy capacity region for different PP constraints. The region corresponding to this scenario is determined through the resolution of the optimization problem presented in (7). A notable trade-off emerges between the information rate sent to the information decoder and the energy rate to the EH receiver. This trade-off becomes apparent as higher EH constraints lead the transmitter to choose a symbol with greater amplitude, consequently reducing the performance of information transfer. It is noteworthy that, for lower amplitude constraints, there is no trade-off between the two objectives. In this regime, the optimal input distribution is binary, maximizing both information and energy transfer simultaneously.

Fig. 3 highlights the impact of the channel on the information-energy capacity region. The comparison reveals a noticeable gap between the two regions, and this discrepancy is primarily attributed to the adverse effects introduced by the lognormal channel. Specifically, we observed that the information energy capacity region of the Gaussian channel outperforms that of the lognormal channel. This gap in performance can be attributed to the inherent characteristics of the lognormal channel, which introduces challenges such as signal attenuation and fluctuations.

V. Conclusion

In this paper, we studied the information-energy capacity region of a SLIPT system over a lognormal-fading channel with nonlinear EH, where the PP, AP, and EH constraints were considered. An expression for the transition probability distribution of the lognormal channel was derived. By using Smith's framework and introducing appropriate Hermite polynomial bases, we proved that the optimal input distribution is discrete with a finite number of mass points. Numerical results of the information-energy capacity region were presented and compared it with AWGN channel conditions. Results show that under low PP constraints the optimal distribution is binary and no trade-off between the information rate and the EH. Further, lognormal fading results in degradation of the information-energy capacity region as compared with AWGN channel conditions.

Appendix A
Proof of Theorem 3

We show that the equality in (15) can not be satisfied on a set of points that has an accumulation point, which indicates that the set Supp(F^*) must be discrete and the optimal input X must be a discrete random variable. We start with the necessary and sufficient conditions for the optimality of F^*. Extending the necessary and sufficient conditions of Corollary 2 to the complex domain, the left-hand side (LHS) of (15) reduces to

$$s(z) = \lambda_1(z-\varepsilon) - \lambda_2(bz\ln(1+cz) - E_{th}) + C - \int p(y|z)\log_2\frac{p(y|z)}{p(y;F^*)}\mathrm{d}y, \quad z \in \mathcal{D}, \tag{16}$$

where the domain $\mathcal{D}$ is defined by $\Re(z) > 0$. The function $s(z)$ is analytic over the complex domain, since the linear function, and the logarithmic function are all analytic. The necessary condition for the optimal input distribution F^* is that $s(z)$ must be zero $\forall z \in$ Supp(F^*). However, from the identity theorem, if the set Supp(F^*) has an accumulation point and the analytic function $s(z) = 0, \forall z \in \mathcal{D}$, then $s(z)$ is necessarily zero over the whole $\mathcal{D}$, and hence, from (16)

$$\int p(y|z)\log_2 p(y;F^*)\mathrm{d}y = -C - \lambda_1(z-\varepsilon) + \lambda_2(bz\ln(1+cz) - E_{th}) + \int p(y|z)\log_2 p(y|z)\mathrm{d}y. \tag{17}$$

A. Conditional Probability of the Channel

The conditional probability $p_{Y|X}(y|x)$ of the lognormal channel is not present in the literature. Hence, we derive $p_{Y|X}(y|x)$, which will be used to derive the properties of

the optimal input distribution. According to (3), the random variable Y of the channel output can be represented as $Y = X_1 + N$, where $X_1 = aR_P h_{1,l} H_T X$, H_T is the lognormal fading, X is the channel input, and N is the AWGN. By using the basic properties of pdfs, the pdf of Y is the convolution of pdfs of X_1 and N. Hence, for a given input X,

$$p_{Y|X}(y|x) = \int_0^{+\infty} p_{X_1|X}(t|x) p_N(y-t)\mathrm{d}t, \tag{18}$$

where $p_{X_1|X}(t|x)$ is the pdf of X_1 for a given input X, and $p_N(t)$ is the pdf of N, respectively. By using the variable transformation from H_T to X_1 in (2), $p_{X_1|X}(x_1|x)$ can be deduced, and hence, the conditional probability in (18) is written as

$$p_{Y|X}(y|x) = \frac{1}{4\pi\sigma_g\sigma_{X_l}} \int_0^{+\infty} \frac{1}{t} \tag{19}$$
$$\times \exp\left(-\frac{\left(\ln\left(\frac{t}{aR_P h_{1,l} x}\right) - 2\mu_{X_l}\right)^2}{8\sigma_{X_l}^2}\right) \exp\left(-\frac{(y-t)^2}{2\sigma_g^2}\right)\mathrm{d}t.$$

By apply the variable transformation $k = \ln\left(\frac{t}{aR_P h_{1,l} x}\right)$ and after several manipulations, we obtain

$$p_{Y|X}(y|x) = \frac{e^{-\frac{y^2}{2\sigma_g^2}}}{4\pi\sigma_g\sigma_{X_l}} \int_{-\infty}^{+\infty} \exp\left(-\frac{(k-2\mu_{X_l})^2}{8\sigma_{X_l}^2}\right) \tag{20}$$
$$\times \exp\left(\frac{aR_P h_{1,l} x e^k}{\sigma_g}\frac{y}{\sigma_g} - \left(\frac{aR_P h_{1,l} x e^k}{\sigma_g}\right)^2\right)\mathrm{d}k.$$

It can be identified that the second exponential term inside the integration is in the form of the generating function of the Hermite polynomial which is $e^{xt-\frac{t^2}{2}} = \sum_{n=0}^{\infty} H_{e_n}(x)\frac{t^n}{n!}$, where $H_{e_n}(x)$ is the Hermite polynomial of n-th kind [21]. Applying this relation, interchanging the order of summation with integration, and with some rearrangements, (20) can be written as

$$p_{Y|X}(y|x) = \frac{e^{-\frac{y^2}{2\sigma_g^2}}}{4\pi\sigma_g\sigma_{X_l}} \sum_{n=0}^{\infty} \frac{1}{n!} H_{e_n}\left(\frac{y}{\sigma_g}\right)\left(\frac{aR_P h_{1,l} x}{\sigma_g}\right)^n$$
$$\times \int_{-\infty}^{+\infty} \exp\left(-\frac{(k-2\mu_{X_l})^2}{8\sigma_{X_l}^2} + nk\right)\mathrm{d}k. \tag{21}$$

The integration in (21) can be identified as a standard result of the integration $\int_{-\infty}^{\infty} \exp\left(-ak^2+bk-c\right)\mathrm{d}k = \sqrt{\frac{\pi}{a}}\exp\left(\frac{b^2}{4a}-c\right)$ where $a = \frac{1}{8\sigma_{X_l}^2}$, $b = \frac{\mu_{X_l}+2n\sigma_{X_l}^2}{2\sigma_{X_l}^2}$, and $c = \frac{\mu_{X_l}^2}{2\sigma_{X_l}^2}$. With simplifications, the final expression can be expressed as

$$p_{Y|X}(y|x) = \frac{e^{-\frac{y^2}{2\sigma_g^2}}}{\sqrt{2\pi\sigma_g^2}} \sum_{n=0}^{\infty} \frac{1}{n!} H_{\mathrm{e}_n}\left(\frac{y}{\sigma_g}\right) K_n^n x^n, \tag{22}$$

where $K_n = aR_P h_{1,l} e^{2(n\sigma_{X_l}^2+\mu_{X_l})}$. Similar to [21], we set $\sigma_g^2 = 1$ to simplify the proof without the loss of generality.

Now, $\log\left(p(y;F^*)\right)$ in (17) is a continuous function of y and is a square integrable with respect to $e^{-y^2/2}$. As such, it can be written in terms of the Hermite polynomials as

$$\log\left(p(y;F^*)\right) = \sum_{m=0}^{\infty} c_m H_{\mathrm{e}_m}(y). \tag{23}$$

Next, using (22), (23), and the orthogonality property of the Hermite polynomials with respect to $e^{-y^2/2}$, i.e.,

$$\int_{-\infty}^{\infty} e^{-y^2/2} H_{\mathrm{e}_m}(y) H_{\mathrm{e}_n}(y) = m!\sqrt{2\pi} \tag{24}$$

if $m = n$ and zero otherwise [19], $\int p(y|z)\log p(y;F^*)\mathrm{d}y$ is expressed as

$$\int p(y|z)\log p(y;F^*)\mathrm{d}y = \sum_{m=0}^{\infty} c_m (K_m z)^m. \tag{25}$$

Let $V_n = f^{(n)}[bx\log(1+cx)](0)$. Then, the Taylor expansion of $bz\log(1+cz)$ is given by

$$bz\log(1+cz) = \sum_{m=0}^{\infty} V_m z^m. \tag{26}$$

Similarly, $\log\left(p(y|z)\right)$ is a continuous function of y and is a square integrable with respect to $e^{-y^2/2}$, and hence, it can be written in terms of the Hermite polynomials as

$$\log\left(p(y|z)\right) = \sum_{m=0}^{\infty} a_m H_{\mathrm{e}_m}(y). \tag{27}$$

Hence, with the use of (22), (27), and the orthogonal property of Hermite polynomial, the term $\int p(y|z)\log p(y|z)\mathrm{d}y$ is written as

$$\int p(y|z)\log p(y|z)\mathrm{d}y = \sum_{m=0}^{\infty} a_m (K_m z)^m. \tag{28}$$

With the use of (25), (26), and (28), Eq. (16) is reduced to

$$\sum_{m=0}^{\infty} c_m (K_m z)^m = \lambda_2\left(\sum_{m=0}^{\infty} V_m z^m - E_{th}\right) - \lambda_1(z-\epsilon)$$
$$- C + \sum_{m=0}^{\infty} a_m (K_m z)^m. \tag{29}$$

Equating the coefficients of z^m, we have

$$\begin{aligned} c_0 &= \lambda_2(V_0 - E_{th}) + \lambda_1\epsilon - C + a_0, \\ c_1 &= \frac{\lambda_2 V_1 - \lambda_1 + a_1 K_1}{K_1}, \\ c_m &= \frac{\lambda_2 V_m + a_m K_m^m}{K_m^m}, \quad \text{for all } m > 1. \end{aligned} \tag{30}$$

By inserting (30) into (23), the following holds

$$p(y;F^*) = e^{\ln(2)\sum_{m=0}^{\infty} c_m H_{\mathrm{e}_m}(y)}. \tag{31}$$

Next, by following similar steps as [19], it can be shown that $p(y;F^*)$ can not be a valid output distribution. Hence, $\mathrm{Supp}(F^*)$ can not have an accumulation point and X^* must be a discrete random variable. This completes the proof.

REFERENCES

[1] M. Z. Chowdhury, M. T. Hossan, A. Islam, and Y. M. Jang, "A comparative survey of optical wireless technologies: Architectures and applications," *IEEE Access*, vol. 6, pp. 9819–9840, Jan. 2018.

[2] P. D. Diamantoulakis, G. K. Karagiannidis, and Z. Ding, "Simultaneous lightwave information and power transfer (SLIPT)," *IEEE Trans. Green Commun. Netw.*, vol. 2, pp. 764–773, Sept. 2018.

[3] V. K. Papanikolaou *et al.*, "Simultaneous lightwave information and power transfer in 6G networks," *IEEE Commun. Mag.*, vol. 62, pp. 16–22, Sept. 2023.

[4] S. Ma, F. Zhang, H. Li, F. Zhou, Y. Wang, and S. Li, "Simultaneous lightwave information and power transfer in visible light communication systems," *IEEE Trans. Wirel. Commun.*, vol. 18, pp. 5818–5830, Sept. 2019.

[5] G. Pan, P. D. Diamantoulakis, Z. Ma, Z. Ding, and G. K. Karagiannidis, "Simultaneous lightwave information and power transfer: Policies, techniques, and future directions," *IEEE Access*, vol. 7, pp. 28 250–28 257, Feb. 2019.

[6] S. Sepehrvand, L. N. Theagarajan, and S. Hranilovic, "Rate-power tradeoff in simultaneous lightwave information and power transfer systems," *IEEE Commun. Lett.*, vol. 25, pp. 1249–1253, Dec. 2021.

[7] A. M. Abdelhady, O. Amin, B. Shihada, and M.-S. Alouini, "Spectral efficiency and energy harvesting in multi-cell SLIPT systems," *IEEE Trans. Wirel. Commun.*, vol. 19, pp. 3304–3318, May. 2020.

[8] M. Liu *et al.*, "Simultaneous mobile information and power transfer by resonant beam," *IEEE Trans. Signal Process.*, vol. 69, pp. 2766–2778, May 2021.

[9] M. Uysal *et al.*, "SLIPT for underwater visible light communications: Performance analysis and optimization," *IEEE Trans. Wirel. Commun.*, vol. 20, pp. 6715 – 6728, May 2021.

[10] A. Chaaban, O. M. S. Al-Ebraheemy, T. Y. Al-Naffouri, and M.-S. Alouini, "Capacity bounds for the gaussian IM-DD optical multiple-access channel," *IEEE Trans. Wirel. Commun.*, vol. 16, pp. 3328–3340, May 2017.

[11] A. Lapidoth, S. M. Moser, and M. A. Wigger, "On the capacity of free-space optical intensity channels," *IEEE Trans. Infor. Theory*, vol. 55, pp. 4449–4461, Sept. 2009.

[12] N. Shanin, H. Ajam, V. K. Papanikolaou, L. Cottatellucci, and R. Schober, "Accurate EH modelling and achievable information rate for SLIPT systems with multi-junction photovoltaic receivers," *ArXiv e-prints*, Aug. 2023. [Online]. Available: arXiv:2308.13848

[13] M. V. Jamali *et al.*, "Statistical studies of fading in underwater wireless optical channels in the presence of air bubble, temperature, and salinity random variations," *IEEE Trans. Commun.*, vol. 66, pp. 4706–4723, Oct. 2018.

[14] L. Yang, X. Song, J. Cheng, and J. F. Holzman, "Free-space optical communications over lognormal fading channels using OOK with finite extinction ratios," *IEEE Access*, vol. 4, pp. 574–584, Jan. 2016.

[15] J. G. Smith, "The information capacity of amplitude- and variance-constrained," *Inf. Control*, vol. 18, pp. 203–219, Apr. 1971.

[16] N. Anous, M. Abdallah, M. Uysal, and K. Qaraqe, "Performance evaluation of LOS and NLOS vertical inhomogeneous links in underwater visible light communications," *IEEE Access*, vol. 6, pp. 22 408–22 420, Mar. 2018.

[17] M. V. Jamali, A. Chizari, and J. A. Salehi, "Performance analysis of multi-hop underwater wireless optical communication systems," *IEEE Photon. Technol. Lett.*, vol. 29, pp. 462–465, Mar. 2017.

[18] N. Khalfet and I. Krikidis, "The capacity of SWIPT systems over rayleigh-fading channels with HPA," in *Proc. IEEE Info. Theory Works. (ITW 2021)*, Kanazawa, Japan, Oct. 2021, pp. 1–6.

[19] R. Morsi, V. Jamali, D. W. K. Ng, and R. Schober, "On the capacity of SWIPT systems with a nonlinear energy harvesting circuit," in *Proc. IEEE Int. Conf. Commun. (ICC 2018)*, Kansas City, USA, May 2018, pp. 1–7.

[20] M. Grant and S. Boyd, "CVX: Matlab software for disciplined convex programming, version 2.1," http://cvxr.com/cvx, Mar. 2014.

[21] J. J. Fahs and I. C. Abou-Faycal, "Using hermite bases in studying capacity-achieving distributions over AWGN channels," *IEEE Trans. Info. Theory*, vol. 58, pp. 5302–5322, May 2012.